

On the sensitivity of the ultrasonic welding process of epoxy- to polyetheretherketone (PEEK)-based composites to the welding force and amplitude of vibrations

Tsiangou, Eirini; de Freitas, Sofia Teixeira; Benedictus, Rinze; Villegas, Irene Fernandez

DOI

[10.1016/j.jcomc.2021.100141](https://doi.org/10.1016/j.jcomc.2021.100141)

Publication date

2021

Document Version

Final published version

Published in

Composites Part C: Open Access

Citation (APA)

Tsiangou, E., de Freitas, S. T., Benedictus, R., & Villegas, I. F. (2021). On the sensitivity of the ultrasonic welding process of epoxy- to polyetheretherketone (PEEK)-based composites to the welding force and amplitude of vibrations. *Composites Part C: Open Access*, 5, Article 100141. <https://doi.org/10.1016/j.jcomc.2021.100141>

Important note

To cite this publication, please use the final published version (if applicable). Please check the document version above.

Copyright

Other than for strictly personal use, it is not permitted to download, forward or distribute the text or part of it, without the consent of the author(s) and/or copyright holder(s), unless the work is under an open content license such as Creative Commons.

Takedown policy

Please contact us and provide details if you believe this document breaches copyrights. We will remove access to the work immediately and investigate your claim.



On the sensitivity of the ultrasonic welding process of epoxy- to polyetheretherketone (PEEK)-based composites to the welding force and amplitude of vibrations

Eirini Tsiangou*, Sofia Teixeira de Freitas, Rinze Benedictus, Irene Fernandez Villegas

Aerospace Structures and Materials Department, Faculty of Aerospace Engineering, Delft University of Technology, Kluyverweg 1, 2629 HS Delft, the Netherlands

ARTICLE INFO

Keywords:

Polymer-matrix composites (PMCs)
Thermoplastic resin
Thermosetting resin
Joints/joining
Ultrasonic welding

ABSTRACT

This paper addresses the sensitivity of the ultrasonic welding process for joining dissimilar composites to variations in either the welding force or amplitude of vibrations. For that, carbon fibre (CF)/epoxy specimens were welded to CF/polyetheretherketone (PEEK) specimens, through a polyetheretherimide (PEI) coupling layer cured with the CF/epoxy material. It was found that reducing either the welding force or the amplitude of vibrations caused an increase in the heating time and maximum temperatures between the coupling layer and CF/epoxy adherend. In addition, local signs of thermal degradation were found in the CF/epoxy adherend even at welding conditions that resulted in the highest strength. However, such alterations were not significant enough to have an apparent effect on the maximum lap shear strength of the welded joints.

1. Introduction

In the last decades the aerospace industry has been showing an increasing interest in thermoplastic composites not only due to their appealing properties like fast processing, high damage tolerance, virtually infinite shelf life and chemical resistance but also because they can be welded. Welding can lead to much shorter assembly times as compared to adhesive bonding in which long curing cycles are normally required, and can eliminate the drilling of holes (which is not composite friendly, as it adds complexity in the manufacturing process and introduces discontinuities in the fiber reinforcement and point loads) as in mechanical fastening [1,2]. Even though welding is primarily used for thermoplastic materials, it can also be applied to join thermoset to thermoplastic composites. Thus, it could, for instance, constitute a good alternative to the mechanical fastening process currently used to attach the thousands of carbon fiber (CF)/polyetheretherketone (PEEK) clips and brackets to the CF/epoxy skin of the Airbus A350 and Boeing 787 aircraft [3].

Thermoset composites can be welded indirectly through a thermoplastic medium. As a common practice, a thermoplastic film, hereafter referred to as coupling layer, is attached on top of the surface of the thermoset composite that needs to be welded. There are several ways to achieve a bond between the coupling layer and the thermoset composite. One is to use a fiber fabric reinforcement partially impregnated with a thermoplastic resin. The rest of the fabric is impregnated with the thermoset resin during the curing process leading to mechanical interlocking as the primary bonding mechanism [4]. Another method is to treat

the thermoplastic film with ultraviolet ozone (i.e. a surface treatment in which contaminations on the surface of the specimens are dissociated after absorbing UV rays) in order to enhance its adhesion with the thermoset composite [5]. Finally, using a thermoplastic film that is partially miscible with the thermoset resin, as in the case of polyetherimide (PEI) and epoxy resins [3,6,7], results in the creation of a gradient interphase, i.e. a gradient transition from one material to the other, during the curing process. This last method is considered a reliable way to bond the thermoplastic coupling layer with the thermoset composite adherend [8].

One of the main challenges when welding advanced thermoset to thermoplastic composites is that in order to melt the thermoplastic matrix high temperatures need to be reached. This could pose a great risk for thermal degradation of the thermoset composite, since those temperatures are generally above its operational temperatures. One way to significantly limit this risk is by generating heat in a very fast manner, to prevent the degradation mechanisms from occurring [5]. Among the well-known thermoplastic composite welding techniques, ultrasonic welding offers the shortest heating times (even less than 500 ms when high welding force and amplitude of vibrations, e.g. 1200 N and 86 μm (peak-to-peak) were chosen) [9], thus it is an excellent candidate for joining the two dissimilar composites. Ultrasonic welding is a joining process based on the introduction of high-frequency and low-amplitude vibrations transverse to the interface to be welded [10,11]. In order to promote local heat generation an energy director (ED), either resin protrusions molded on the adherends or a loose neat resin film, is commonly placed at the welding interface [12]. Ultrasonic heat generation is based

* Corresponding author.

E-mail address: E.Tsiangou@tudelft.nl (E. Tsiangou).

on surface friction and viscoelastic heating [13,14], which are mainly driven by the static force and by the amplitude of the vibrations applied during the welding process [15]. A combination of high welding force and high amplitude of vibrations (in this context the highest values in which the maximum consumed power does not exceed the limits of the specific welding machine in use) leads to short heating times, even below 500 ms, which, as indicated before, is regarded as beneficial when welding thermoset to thermoplastic composites.

The suitability of ultrasonic welding for welding thermoplastic and thermoset composites has been shown in a number of studies. A study by Villegas and van Moorlegem [3] on ultrasonic welding of CF/epoxy and CF/PEEK adherends through a PEI coupling layer showed a promising average lap shear strength (LSS) of 28.6 ± 2.3 (average \pm standard deviation) MPa. Lionetto et al. [16] presented a comparison between ultrasonic and induction welding as potential solutions to join CF/epoxy specimens through poly-vinyl-butyl coupling layers. That study revealed superior mechanical performance and overall weld quality of the ultrasonically welded specimens. The authors of the present study investigated in [8] the possibility of ultrasonically welding CF/epoxy to CF/PEI specimens solely through the PEI coupling layer. The conclusion was that an ED is required at the interface to help generate heat locally, without risking excessive bulk heating and thermal degradation in any of the adherends. Moreover, the LSS of welded CF/epoxy to CF/PEI specimens through a PEI film acting as ED plus a 60 μm -thick PEI coupling layer was found to be similar to that of reference co-cured CF/epoxy and CF/PEI composites. In a later study [17], the authors of this study assessed the effects of the material of the ED and the thickness of the PEI coupling layer on ultrasonic welding of CF/epoxy to CF/PEEK adherends. It was shown that, for that specific material combination, a 250 μm -thick PEI coupling layer results in higher LSS than the 60 μm -thick coupling layer. In particular, the LSS of the specimens with a 250 μm -thick layer was comparable to the LSS of reference CF/PEEK welded specimens. Compared to the study in [8] in which a 60 μm -thick PEI coupling layer was sufficient to produce welds with acceptable mechanical performance, the PEEK matrix has a higher melting temperature than the softening temperature of PEI, which increases the risk of thermal degradation of the epoxy resin. Finally Villegas and Rubio showed in their study [5] that using a combination of high welding force and high amplitude of vibrations to join CF/epoxy to CF/PEEK adherends, resulted in short heating times and consequently in absence of thermal degradation in the CF/epoxy adherend. On the contrary, long heating times induced by selecting a low welding force and low amplitude of vibrations caused visible signs of thermal degradation in the CF/epoxy adherend.

All the above-mentioned studies on ultrasonic welding of thermoplastic to thermoset composites were carried out using the highest welding force and amplitude combinations allowed by the ultrasonic welder (i.e., those in which the maximum consumed power did not exceed the limit of the machine) combined with an optimum vibration time, defined as that which lead to maximum weld strength. Studies on the flexibility of the process with regards to variations on any of those three parameters are still scarce. They are however important in order to establish the robustness of the process, especially when considering future industrial applications. In a recent study [18], we investigated the sensitivity of ultrasonic welding of CF/epoxy to CF/PEEK composites to the heating time. It was shown that high-strength welds could be obtained for a relatively wide range of heating times, indicating that ultrasonic welding of dissimilar composites is not as sensitive to the heating time as originally suspected. It is however still unknown whether the process could also allow some flexibility regarding variations on the welding force and the vibrational amplitude.

Therefore, the main focus of the present study is to determine the sensitivity of the ultrasonic welding process of CF/epoxy to CF/PEEK composites to variations in the welding force and the amplitude of vibrations, in particular a decrease from the high values used for both parameters in previous studies. Firstly, the effect of a decrease in either

Table 1
Thermal properties of the PEI and PEEK resins.

Material	T_g (°C)	T_m (°C)
PEI	215 ^a	–
PEEK	143 ^b	343 ^b

^a Technical datasheet of LITE PEI.

^b Technical datasheet of Victrex PEEK.

the welding force or the vibration amplitude on the welding process was assessed through i) analyzing the welding output, i.e., dissipated power and displacement of the sonotrode, provided by the welder and ii) measuring the temperature in between the coupling layer and the CF/epoxy material, since the latter is the one at higher risk of thermal degradation. Secondly, the effects of a decrease in the force or the amplitude on (i) the maximum achievable LSS and (ii) in the heating time resulting in the highest strength. The mechanical performance of the welds was assessed through single-lap shear tests and fractographic analysis.

2. Experimental procedure

2.1. Materials and manufacturing

In this study, Cetex® CF/PEEK (carbon fiber/polyetheretherketone) prepreg with a 5-harness satin fabric reinforcement, manufactured by TenCate Advanced Composites (the Netherlands) was used as the TPC adherend. Its thermal properties can be found in Table 1. CF/PEEK prepreg plies arranged in a $[0/90]_{3s}$ stacking sequence were consolidated in a hot-platen press at 385 °C and 1 MPa for 30 min. The thickness of the consolidated laminates was 1.88 ± 0.01 mm (average \pm standard deviation, measured at 6 locations).

A T800S/3911 unidirectional CF/epoxy prepreg provided by TORAY (Japan) was used as the TSC adherend. Individual plies were manually laid up in a $[0/90]_{2s}$ configuration. A 175 ± 2 μm -thick PEI film (10 measurement locations on the as-received film) from LITE (Germany) was used as the coupling layer. The PEI material was chosen due to its partial miscibility with most epoxy resins [6] as well as miscibility with the PEEK resin at the melting temperature of the latter [19]. It should be noted that co-curing the 175 μm -thick coupling layer on only one surface of the TSC laminate resulted in post-cure warpage, possibly because of the different thermal expansion coefficient of the CF/epoxy and PEI materials. Hence, the PEI film was co-cured to both outer surfaces of the CF/epoxy laminates, leading to flat laminates. Annealing would be an interesting alternative to release some of the residual stresses that result in warpage of the laminates. However, it should be further investigated to which extent annealing would solve the problem. Prior to its application on the pre-preg stack, the PEI coupling layer was degreased with isopropanol. The thermal properties of the PEI film can be found in Table 1. The CF/epoxy laminate with the PEI films was cured in an autoclave at 180 °C and 7 bars for 120 min, according to the specifications of the manufacturer. To ensure smooth surfaces on both sides of the laminate, an aluminum caul plate was used on the side of the vacuum bag. The final thickness of the CF/epoxy/PEI laminate was 2.46 ± 0.01 mm (average \pm standard deviation, measured at 6 locations). In our previous study [8] we found that an approximately 25 μm -thick gradient epoxy/PEI interphase was formed between these epoxy and PEI materials during the curing process. The gradient interphase consisted of epoxy spheres dispersed in the PEI resin. The diameter of these spheres was smaller closer to the PEI film than in the region with high epoxy resin content. More information on how the interphase was developed and its main features can be found in [8].

CF/PEEK and CF/epoxy/PEI adherends with dimensions 25.4 mm \times 106 mm were cut from the laminates using a water-cooled circular diamond saw. The CF/PEEK adherends were cut with their longitudinal direction parallel to the main apparent orientation of the fibers. The

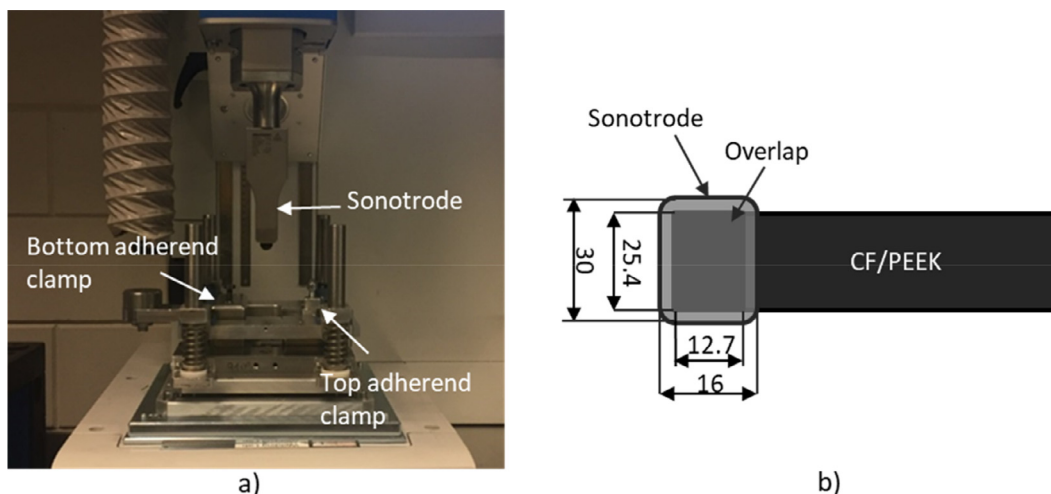


Fig. 1. a) Custom made welding jig and b) position of the sonotrode with respect to the top, CF/PEEK adherend. Dimensions are in mm. Dimensions are not to scale.

CF/epoxy/PEI adherends were cut with their longitudinal direction parallel to the 0° fibers on the outer surfaces of the laminate.

2.2. Welding process

Individual specimens were welded with a HiQ DIALOG SpeedControl ultrasonic welder (Herrmann Ultraschal, Germany) using the custom-made clamping jig shown in Fig. 1a. The jig comprised two separate clamping systems for the top and bottom adherend and was designed to minimize bending of the top adherend during the welding process. Displacement-controlled welding was used, which means that the vibration time was indirectly controlled by stopping the process at specific displacements of the sonotrode. The specimens were welded in a single-lap configuration with a 12.7 mm long and 25.4 mm wide overlap and using a $250 \pm 2 \mu\text{m}$ -thick (based on 10 different measurements) PEEK film provided by Victrex (the Netherlands) as energy director (ED). The ED was cut 4 mm longer than the overlap and attached on the CF/epoxy specimen with adhesive tape. A standard rectangular sonotrode with contact surface dimensions 30 mm \times 16 mm was utilized. Note that the contact surface of the sonotrode was slightly bigger than the overlap (i.e., 25.4 mm \times 12.7 mm) in order to ensure welding of the complete overlap (see Fig. 1b). Five welding combinations of welding force and peak-to-peak amplitude of vibrations were considered, namely 1200 N/86 μm , 1200 N/70 μm , 1200 N/60 μm , 800 N/86 μm and 400 N/86 μm . 1200 N and 400 N were the highest and lowest force values that could be selected to stay within the operating limits of the machine, i.e., 5000 W maximum power. Likewise, 86 μm and 60 μm were the highest and lowest peak-to-peak amplitude of vibrations that could be selected. The middle values of 800 N and 70 μm were selected for completion. The consolidation force was the same as the welding force for each configuration and the consolidation time was fixed to 4 s.

2.3. Process characterization

Output provided by the welder in terms of consumed power and vertical displacement of the sonotrode throughout the process was used to evaluate the effect of changes in the welding force and amplitude of vibration on the welding process. Furthermore, temperature measurements at the interface between the coupling layer and the CF/epoxy adherend were performed in order to evaluate effects on the way heat was transferred from the welding interface to the CF/epoxy adherend. For this purpose, K-type thermocouples with 100 μm diameter were placed between the coupling layer and CF/epoxy laminate prior to the co-curing process. After the co-curing process, specimens were cut from the laminate such that they had one thermocouple with its tip located

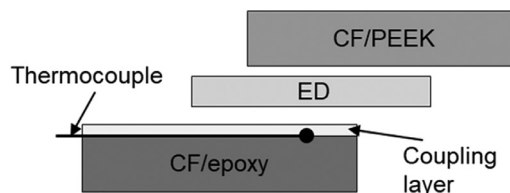


Fig. 2. Schematic representation of the welding stacking sequence and the thermocouple location in CF/epoxy adherends. Dimensions are not to scale.

in the center of the overlap (see Fig. 2). A data acquisition system built into the ultrasonic welder was used to monitor the temperature at a sampling rate of 1000 Hz. The temperature was measured in at least three specimens per combination of welding force and amplitude. Note that the results of the temperature measurements could not be directly related to the power consumed during the welding process (in particular, energy or integral of the power over the welding time) since it not only computes the actual power invested in the creation of the weld but also power losses to the surroundings (adherends, welding jig and base).

2.4. Mechanical testing and fractography

The mechanical performance of the welded specimens was assessed through single lap shear tests (ASTM D 1002 standard) performed in a Zwick 250 kN universal testing machine. The apparent lap shear strength (LSS) of the joints was calculated as the maximum load measured during testing divided by the overlap area. Note that even when unwelded areas were present, the whole overlap was chosen to calculate the lap shear strength since welding the whole overlap was the target. At least five specimens were welded per combination of welding force and amplitude to determine an average LSS value and its corresponding standard deviation. Images of matching fracture surfaces taken via a digital camera were used for the fractographic analysis of the welded joints after mechanical testing. An optical microscope (Zeiss Axiovert 40) was used for cross-sectional analysis of as-welded specimens.

3. Results

3.1. Process characterization

Changes in either the welding force or amplitude of the vibrations are expected to have an impact on the welding process and subsequently the welding output. As part of this output, Fig. 3 shows representative power and displacement curves of specimens welded with different

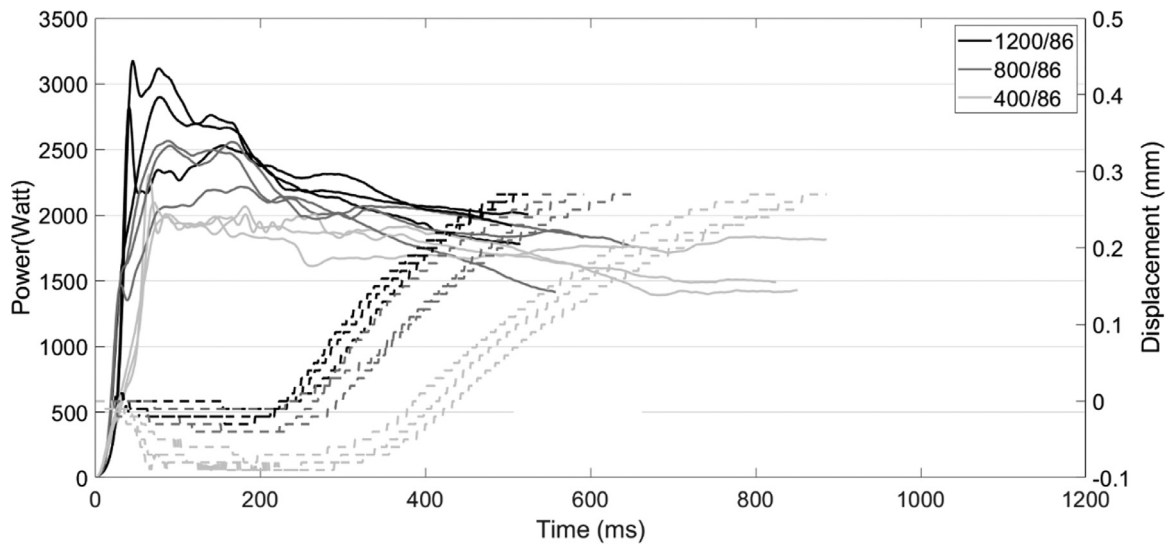


Fig. 3. Representative power (solid lines) and displacement (dashed lines) curves of the 1200/86, 800/86 and 400/86 configurations (3 welded specimens per configuration). All specimens were welded up to 0.28 mm displacement.

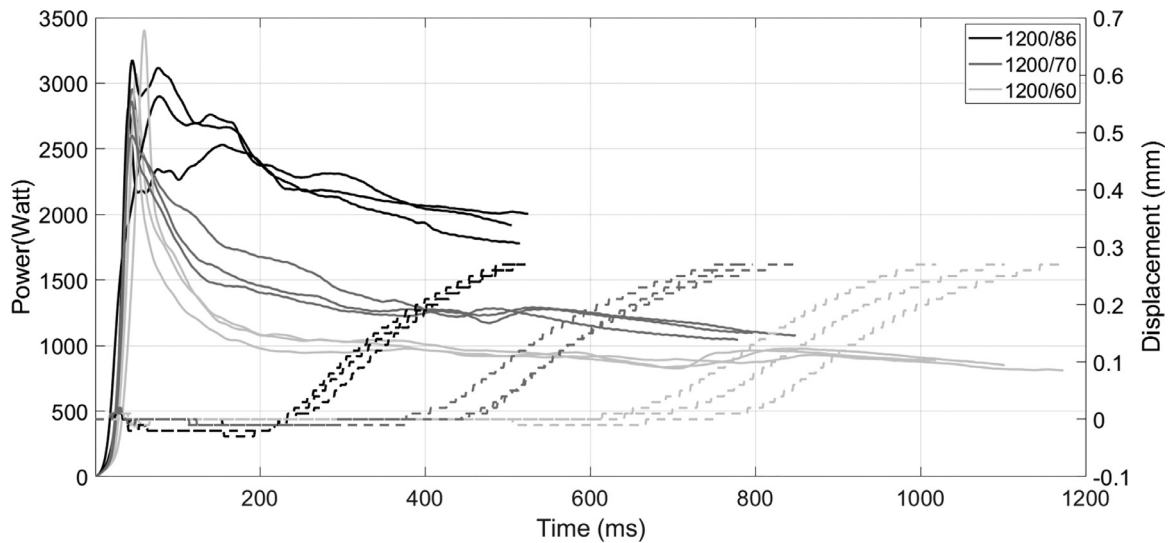


Fig. 4. Representative power (solid lines) and displacement (dashed lines) curves of the 1200/86, 1200/70 and 1200/60 configurations (3 welded specimens per configuration). All specimens were welded up to 0.28 mm displacement.

welding forces and the same amplitude of vibrations (86 μm peak-to-peak). A first observation is that the initial constant value of the displacement prior to the onset of the squeeze, most likely non-Newtonian, flow dropped below 0 mm when the welding force was lower than 1200 N. In particular, the initial displacement was around -0.08 mm in the 400/86 configuration; and between -0.02 mm and -0.04 mm in the 800/86 configuration. The time until the onset of the squeeze flow was similar in the 1200/86 and 800/86 configurations, whilst in the 400/86 configuration it was approximately 100 ms longer. After this onset, the displacement generally increased at a slower pace with decreasing force. Regarding the power consumed during the welding process, a relatively high variability and no clear trend on the effect of decreasing welding force could be observed. The observed variability, which probably resulted in masking of any potential trends, is attributed to variations in the microscopic contact between ED and adherends which would lead to variations in the amount of material initially welded and hence the magnitude of the power peak.

Fig. 4 shows representative power and displacement curves of specimens that were welded with different amplitude of vibrations and the same welding force (1200 N). As seen in this figure, the time un-

til the onset of the downward displacement of the sonotrode, i.e. the time until squeeze flow occurs at the welding interface [15], significantly increased with decreasing amplitude. In particular, the time until the displacement onset increased from an average of around 200 ms in the 1200/86 configuration to around 450 ms in the 1200/70 configuration and to around 700 ms in the 1200/60 configuration. Note that the notation F/A refers to a welding process in which the welding force amounted to "F" N and the peak-to-peak amplitude amounted to "A" μm . After its onset, the displacement increased at a slower pace for decreasing amplitude, i.e., lower squeeze-flow rate for decreasing amplitude. Regarding the evolution of the power consumed during the process, the main difference was that the level at which the power stabilized after a first pronounced power peak(s) was lower for decreasing amplitude of vibrations.

Fig. 5 and Fig. 6 illustrate the temperature evolution at the interface between the PEI coupling layer and the CF/epoxy adherend in configurations welded with different welding forces and different amplitudes, respectively. Regarding changes in the welding force, in the 1200/86 and 400/86 configurations the temperature increased at a similar pace. However, the temperature in the 800/86 configuration increased sig-

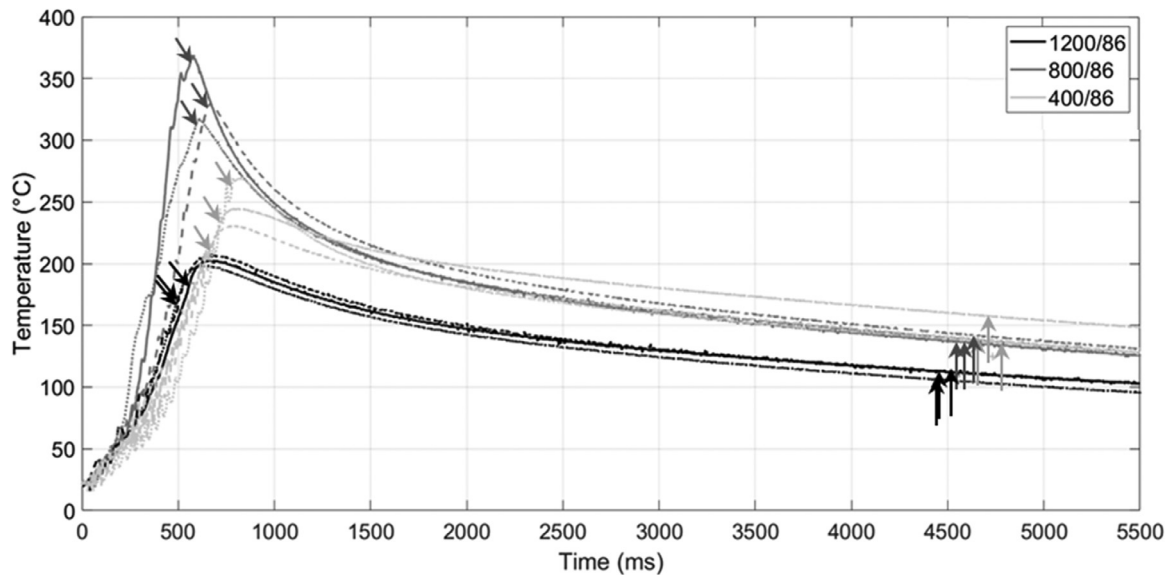


Fig. 5. Effect of decreasing force on temperature evolution at the interface between the PEI coupling layer and CF/epoxy adherend (three welding specimens per configuration, up to 0.28 mm displacement in the 1200/86 and 800/86 cases, up to 0.18 mm in the 400/86 case). Diagonal arrows indicate the end of the vibration. Vertical arrows indicate the end of the welding process (i.e., 4000 ms-long consolidation after the end of the vibration).

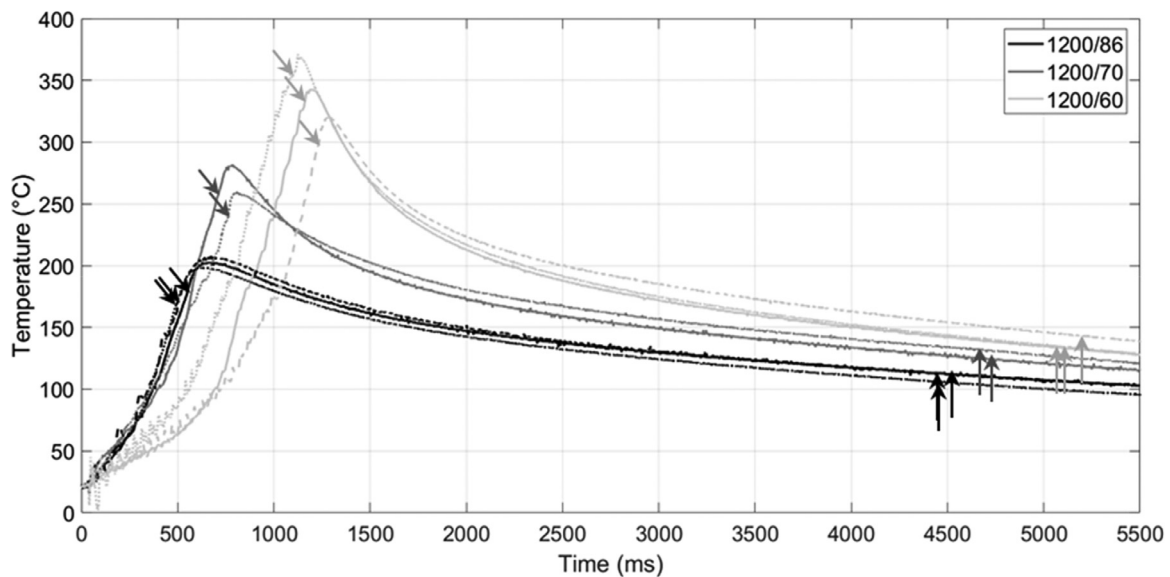


Fig. 6. Effect of decreasing amplitude on temperature at the interface between PEI coupling layer and CF/epoxy adherend (three welding specimens per configuration, up to 0.28 mm in all cases). Diagonal arrows indicate the end of the vibration. Vertical arrows indicate the end of the welding process (i.e., 4000 ms-long consolidation after the end of the vibration). Note that the third measurement for the 1200/70 case contained significant noise and has not been included for clarity.

Table 2
Average temperatures reached in each configuration.

Configuration	d (mm)	T (average \pm stdv, °C)
1200/86	0.28	203 \pm 4
1200/70	0.28	274 \pm 18
1200/60	0.28	338 \pm 24
800/86	0.28	339 \pm 27
400/86	0.20	254 \pm 19

nificantly faster. Regarding changes in the amplitude of vibrations, the temperature increased at a similar rate in the 1200/86 and 1200/70 configurations. In the 1200/60 configuration the temperature increased generally at a slower pace than the other two configurations. The maximum temperatures reached in all cases are found in Table 2. These maximum values were obtained when welding up to 0.28 mm displacement

(1200/86, 800/86, 1200/70 and 1200/60 configurations) and 0.18 mm displacement (400/86 configuration), which, as shown in the next subsection, are the values beyond the displacement that resulted in the maximum average LSS (hereafter referred to as d_{ms}), but that resulted in the most significant differences in LSS. Note that in all cases the maximum temperatures were reached moments after switching off the vibrations, which is consistent with the fact that the temperatures measured resulted from heat conduction through the PEI coupling layer.

3.2. Mechanical performance

Fig. 7 shows the LSS evolution versus the displacement of the sonotrode for configurations welded with different welding forces. Note that in our previous study [18], displacement values between 0.2 and 0.28 mm were considered to be within the processing window for weld-

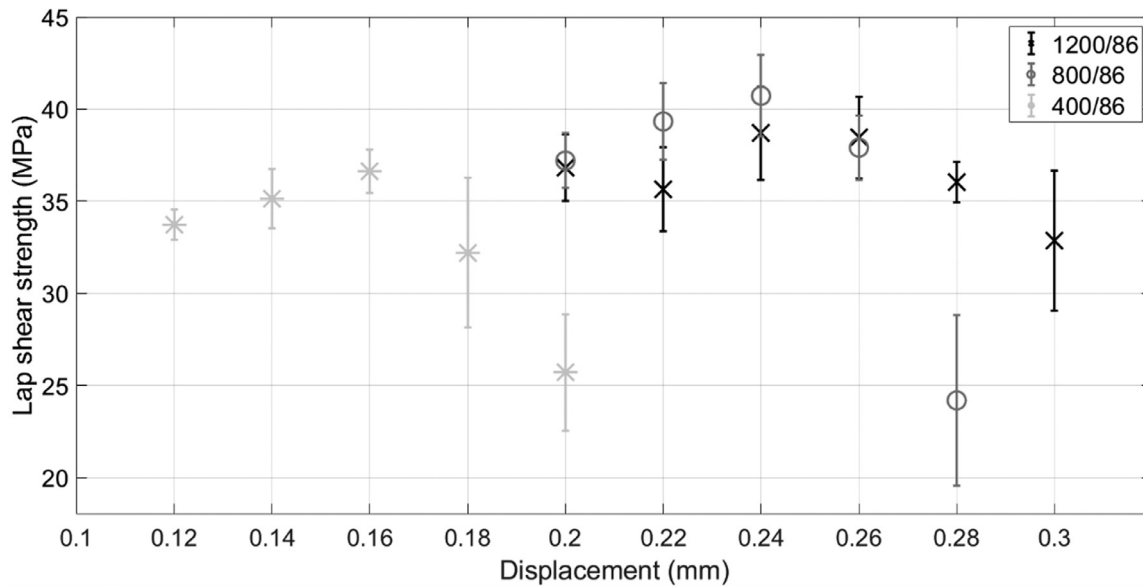


Fig. 7. Evolution of the LSS versus displacement of the sonotrode in the 1200/86, 800/86 and 400/86 configurations.

Table 3

Displacement values for maximum LSS, (d_{ms}), maximum LSS (LSS_{max}), corresponding heating times (t_{ms}) and ANOVA results that determined the d_{ms} range in each configuration. Note that in ANOVA the F value indicates whether the variance between the means of two populations is significantly different. The p value is the probability the results could have happened by chance. The hypothesis that the results were significantly different was rejected when the p value was lower than 0.05.

Configuration	d_{ms} (mm)	LSS_{max} (average \pm stdv, MPa)	t_{ms} (average \pm stdv, ms)	ANOVA results
1200/86	0.24–0.26	38.7 ± 2.2	$467 \pm 57 - 494 \pm 57$	$F(1,14)= 0.6,$ $p = 0.44$
1200/70	0.24–0.26	39.2 ± 3.6	$717 \pm 37 - 754 \pm 30$	$F(1,8)= 0.00,$ $p = 0.99$
1200/60	0.24–0.26	37.9 ± 4.6	$1053 \pm 45 - 1080 \pm 47$	$F(1,10)= 0.33, p = 0.57$
800/86	0.22–0.26	40.2 ± 2	$471 \pm 12 - 543 \pm 17$	$F(2,12)= 1.63, p = 0.23$
400/86	0.14–0.16	36.6 ± 1.2	$571 \pm 18 - 604 \pm 16$	$F(1,8)= 2.7,$ $p = 0.13$

ing same type of adherends as in the current study and according to the 1200/86 configuration. As seen in this figure, decreasing welding forces shifted the process towards lower displacement values. This shift was particularly significant in the 400/86 configuration. The maximum average LSS values and corresponding displacements that were determined using analysis of variance (ANOVA) (i.e., d_{ms}) can be found in Table 3. In both the 800/86 and the 400/86 configurations the LSS drop after the maximum (at 0.28 mm displacement for 800/86 and at 0.18 mm displacement for 400/86) was more pronounced than in the 1200/86 configuration.

The effect of changing the amplitude of vibrations on the average LSS can be seen in Fig. 8 which represents LSS data for different sonotrode displacement values in the 1200/86, 1200/70 and 1200/60 configurations. As shown in this figure, the LSS values for all three configurations were practically overlapped for displacement values up to 0.26 mm. The maximum average LSS values were achieved in all configurations at 0.24 mm and 0.26 mm according to ANOVA (see Table 3). After 0.26 mm the LSS drop was much more pronounced for the 1200/70 and 1200/60 configurations than for the 1200 N/86 configuration.

Table 3 also shows the range of the heating times corresponding to the displacement values resulting in the maximum LSS (see Figs. 7 and 8) as provided by the ultrasonic welder. Decreasing the welding force while keeping the amplitude constant resulted in a moderate increase of the heating time, namely less than 10% time increase by decreasing the welding force from 1200 to 800 N and an additional 20% time increase by further decreasing the welding force from 800 to 400 N. Decreasing

the amplitude while keeping the welding force constant significantly increased the heating time needed to reach the maximum LSS, namely around 50% time increase by decreasing the amplitude from 86 to 70 μm and a further 40–50% time increase by further decreasing the amplitude from 70 to 60 μm .

3.3. Fractography

The fracture surfaces of tested samples were used to better understand the evolution of the LSS. Fig. 9 presents fracture surfaces of 1200/86 specimens welded at different displacement values. For all the displacement values considered in this study, the predominant type of failure was first-ply failure in the CF/PEEK adherend. At 0.24 mm the specimens presented unwelded areas covering around 6% of the overlap. Above 0.26 mm, failure also occurred in the CF/epoxy adherend. When the welding force was decreased to 800 and further to 400 N (Fig. 10) unwelded areas could not be found at d_{ms} . In the 800/86 configuration, specimens welded at d_{ms} (0.22 mm and 0.26 mm) featured a combination of first-ply failure in the CF/PEEK and in the CF/epoxy adherend. In the 400/86 configuration, specimens welded at d_{ms} (0.14 mm and 0.16 mm) featured first-ply failure in the CF/PEEK adherend as well as porosity and matrix failure (predominantly at the edges of the overlap and covering approximately 50% of its total surface). Increasing the displacement to 0.28 mm and to 0.18 mm in the 800/86 and 400/86 config-

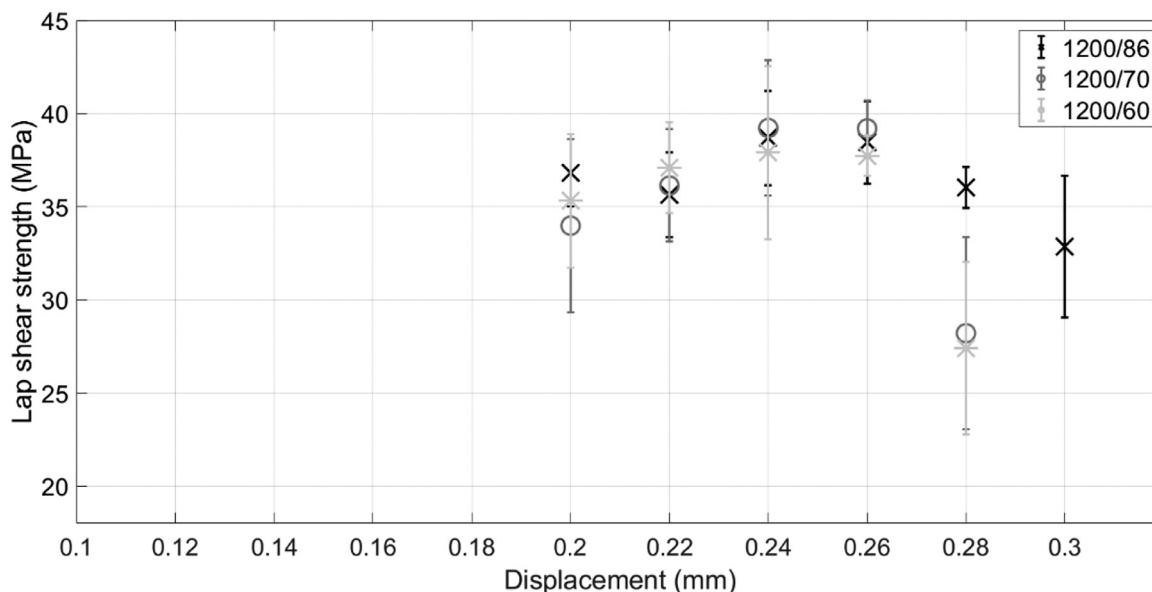


Fig. 8. Evolution of the LSS versus displacement of the sonotrode in 1200/86, 1200/70 and 1200/60 configurations.

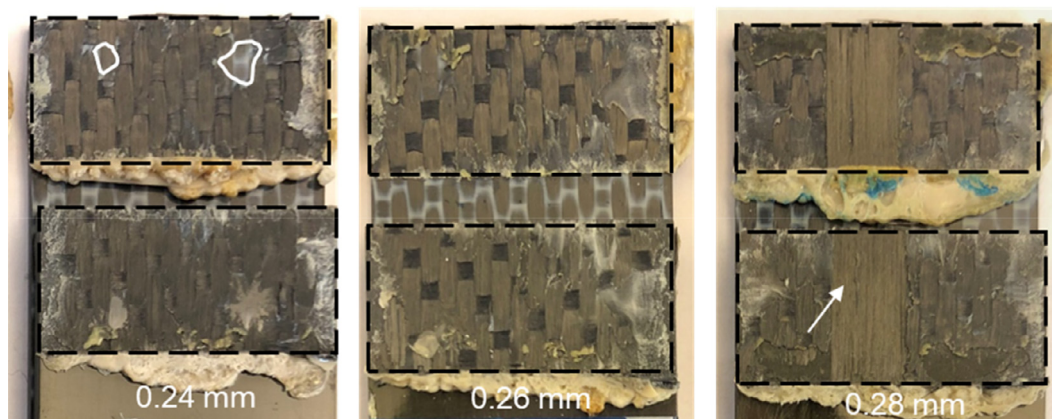


Fig. 9. Representative matching fracture surfaces (CF/PEEK adherend at the top and CF/epoxy adherend at the bottom) of 1200/86 specimens welded at different displacement values. The 0.24 mm and 0.26 mm displacements correspond to the maximum weld strength. The welded overlap is highlighted by the dashed lines. The highlighted areas indicate unwelded areas. The arrows point at failure in the CF/epoxy adherend.

urations, respectively, resulted in predominant failure in the CF/epoxy adherend.

Decreasing the amplitude while keeping the welding force at 1200 N (Fig. 11) resulted in unwelded areas at 0.24 mm (around 6% and 10% of the overlap in the 1200/70 and 1200/60 configurations, respectively), similarly to the 1200/86 configuration. More importantly, decreasing the amplitude resulted in local failure in the CF/epoxy adherend even at d_{ms} values, i.e., 0.24 and 0.26 mm. Further increasing the displacement to 0.28 mm shifted the predominant failure locus to the CF/epoxy adherend.

3.4. Cross-sectional analysis

Fig. 12 shows cross-sectional micrographs from approximately the center of the overlap of specimens corresponding to each force/amplitude configuration. In all cases the specimens were welded at a displacement value that resulted in maximum LSS. The thickness of the weld line (defined as the resin-rich area between the two composite adherends) was $127 \pm 16 \mu\text{m}$, $116 \pm 14 \mu\text{m}$, $125 \pm 16 \mu\text{m}$, $128 \pm 13 \mu\text{m}$ and $126 \pm 11 \mu\text{m}$ in the 1200/86, 1200/70, 1200/60, 800/86 and 400/86 configuration, respectively. The thickness of the weld line was

hence lower than the initial thickness of both the PEEK ED ($250 \mu\text{m}$) and of the PEI coupling layer ($175 \mu\text{m}$), individually. Moreover, in all cases, the weld line was composed of two distinct bands of roughly comparable thicknesses displaying different shades of grey. The dark grey band was identified as PEI whilst the light grey band was identified as PEEK.

4. Discussion

In previous work we looked into ultrasonic welding of CF/PEEK and CF/epoxy composites through a PEI coupling layer at high welding force and high amplitude values [3,17,18]. This procedure was based on the hypothesis that the welding process needs to be as fast as possible (accomplished by using high force and high amplitude) to prevent the occurrence of thermal degradation in the CF/epoxy adherend [5]. This would occur through a two-fold mechanism: i) short welding times can limit the amount of heat transferred to the CF/epoxy adherend across the coupling layer; and ii) short welding times would not allow for thermal degradation reactions to occur even when the material is exposed to high temperatures. In our previous study [18] we showed that, for a combination of high force and high amplitude, the process offers some

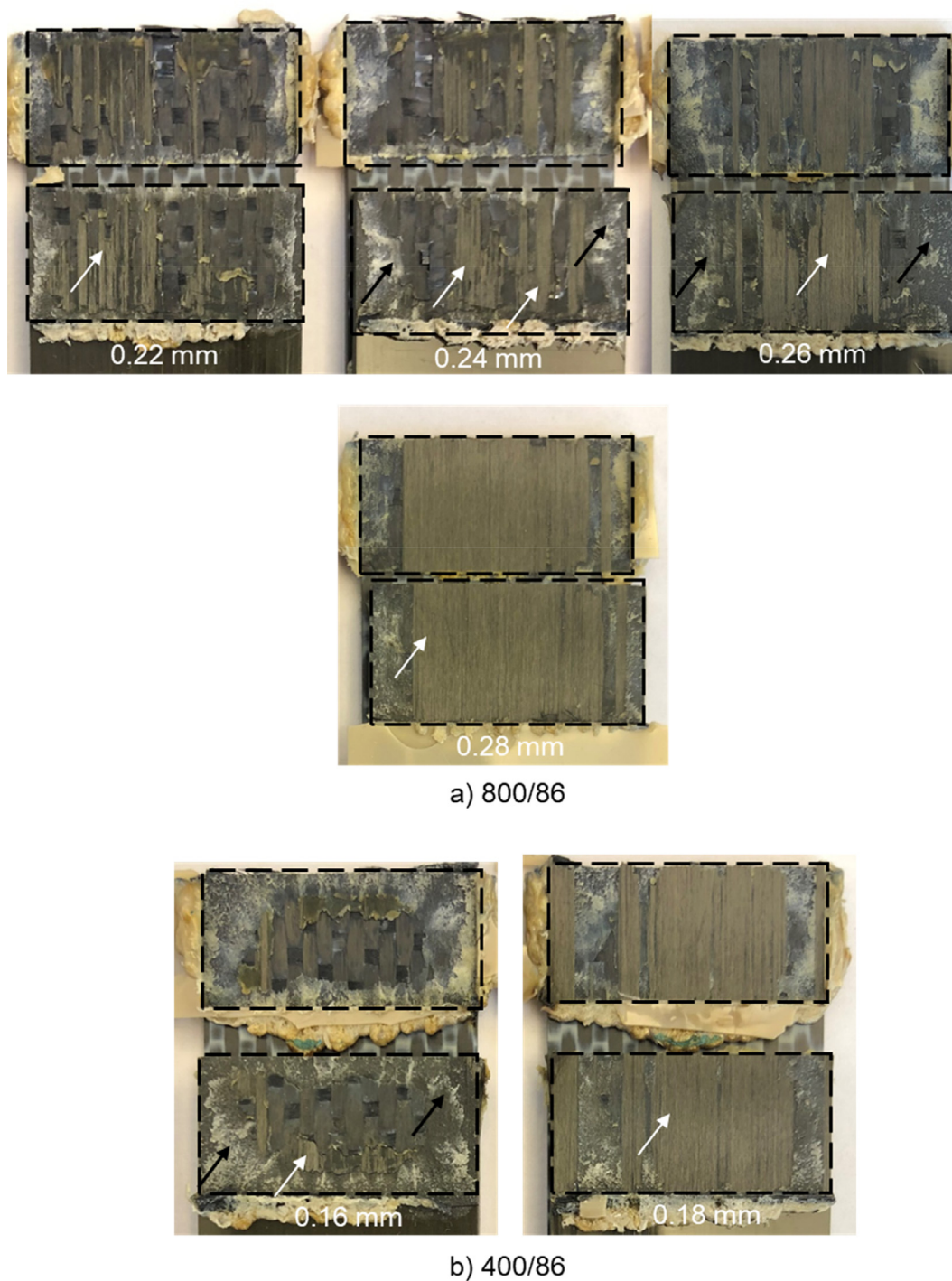


Fig. 10. Representative matching fracture surfaces (CF/PEEK adherend at the top and CF/epoxy adherend at the bottom) of a) 800/86 specimens and b) 400/86 specimens welded at different displacement values. The 0.22, 0.24 and 0.26 mm in a) and 0.16 mm in b) correspond to the maximum weld strength. The welded overlap is highlighted by the dashed lines. The white arrows point at failure in the CF/epoxy adherend. The black arrows point at the areas with porosity.

flexibility in terms of heating time, with a processing interval of around 170 ms width. The question posed in the present paper is whether the process also offers some flexibility in terms of variations (i.e., decrease) of either the welding force or the amplitude.

4.1. Welding force variations (welding at d_{ms})

Decreasing the welding force from 1200 N to 800 N at a high vibration amplitude (86 μ m) did not significantly affect the maximum

achievable LSS (see ANOVA results in Table 4), which is consistent with no significant changes in the heating times resulting in LSS_{max} , either (Table 3). It did however cause changes in the way the welds failed: from first-ply failure exclusively in the CF/PEEK adherend to also local first-ply failure in the CF/epoxy adherend (Fig. 10a). Firstly, the insensitivity of the heating time to the change in the welding force was surprising considering prior research [12] in which the effect of the welding force on the heating time was found to be very significant. That was mostly attributed to the effect of the welding force on the contact at microscopic

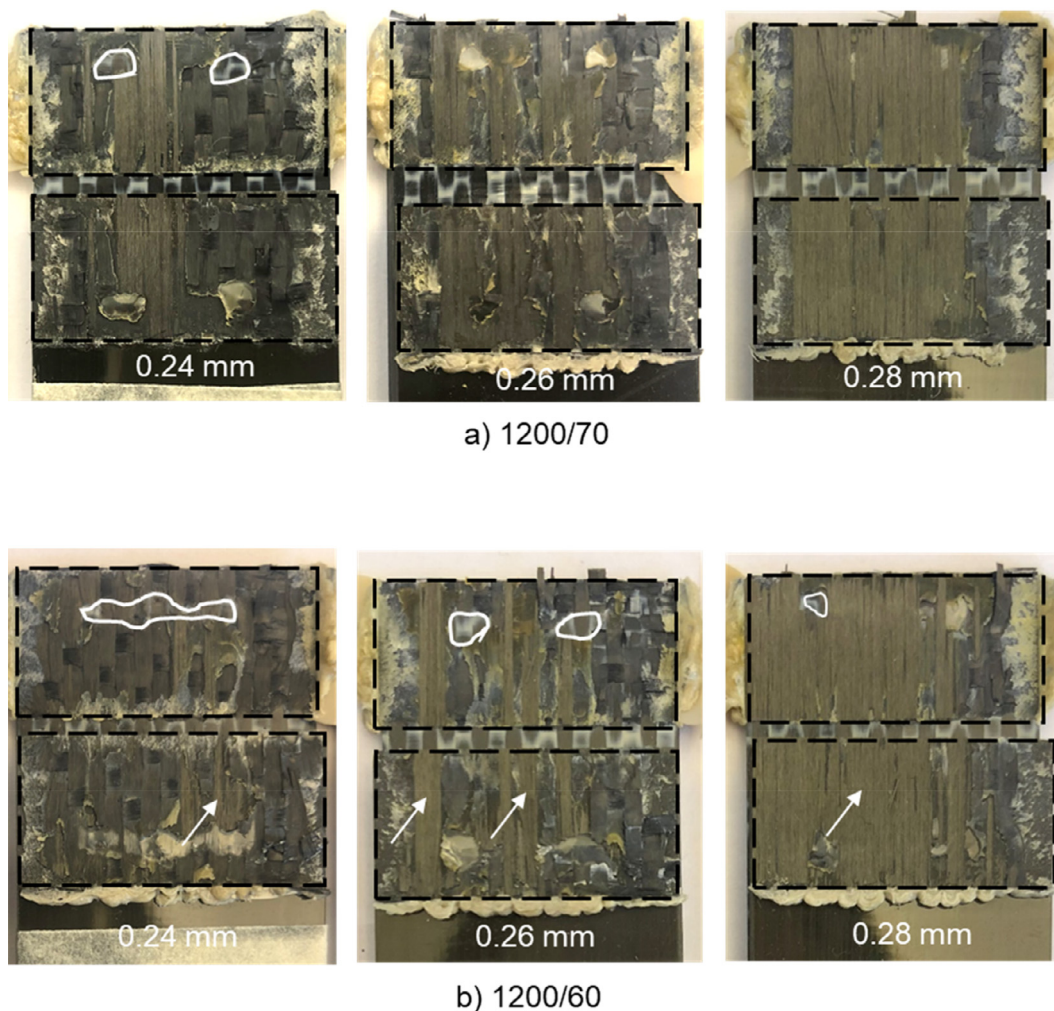


Fig. 11. Representative matching fracture surfaces (CF/PEEK adherend at the top and CF/epoxy adherend at the bottom) of a) 1200/70 specimens and b) 1200/60 specimens, welded at different displacement values. The 0.24 mm and 0.26 mm displacements correspond to the maximum weld strength. The welded overlap is highlighted by the dashed lines. The highlighted areas indicate unwelded areas. The arrows point at failure in the CF/epoxy adherend.

Table 4
Analysis of variance (ANOVA) of maximum LSS values relative to the 1200/86 configuration.

Configuration	Results
1200/70	$F(1,12)= 0.11, p = 0.7$
1200/60	$F(1,15)= 0.21, p = 0.7$
800/86	$F(1,14)= 1.77, p = 0.2$
400/86	$F(1,12)= 3.64, p = 0.08$

level between ED and adherends and hence on friction between the two. In the particular configuration studied in the present paper, however, the higher compliance of the ED-coupling layer interface could result in a significantly lower effect of the force in the heating time. Secondly, the occurrence of local failure in the CF/epoxy adherend is consistent with the decrease in interlaminar strength associated with the occurrence of thermal degradation [20] linked to the higher temperatures registered at the interface between the coupling layer and the CF/epoxy adherend in the 800/86 configuration. Indeed, by superimposing the heating times resulting in LSS_{max} (Table 3) to the temperature graphs in Fig. 5, one can see that the temperature in the 800/86 configuration could be expected to reach around 280 °C at the d_{ms} , while it would be significantly lower, around 150 °C, in the 1200/86 configuration. Nevertheless, the

occurrence of thermal degradation in these specimens welded at d_{ms} was apparently small enough to not have a measurable impact on the maximum achievable LSS.

A further decrease in the welding force to 400 N caused a moderate decrease in the maximum achievable LSS, which is consistent with the longer heating times resulting in LSS_{max} . According to the results of our statistical analysis (see Table 4), this LSS value was however not significantly different from that obtained in the 1200/86 configuration. Fracture surfaces (Fig. 10b) showed increased occurrence of matrix failure linked to porosity at the edges of the overlap, whilst first-ply failure in the CF/PEEK adherend, and occasionally in the CF/epoxy adherend, remained the main sources of failure in the center of the overlap. Porosity at the edges of the overlap seemed to be linked to the combination of high temperature and low pressure due to the lower consolidation force. In fact, the temperature measured in the center of the overlap was higher than that in the 1200/86 configuration (Fig. 5). On top of that, as known from previous work [14], the temperature at the edges of the overlap can be expected to be higher than that in the center of the overlap owing to increased slippage.

It is interesting to note that decreasing the welding force did not show a consistent trend on the temperatures measured at the interface between the coupling layer and the CF/epoxy adhered (Fig. 5). On one hand, decreasing the force from 1200 N to 800 N caused an increase in

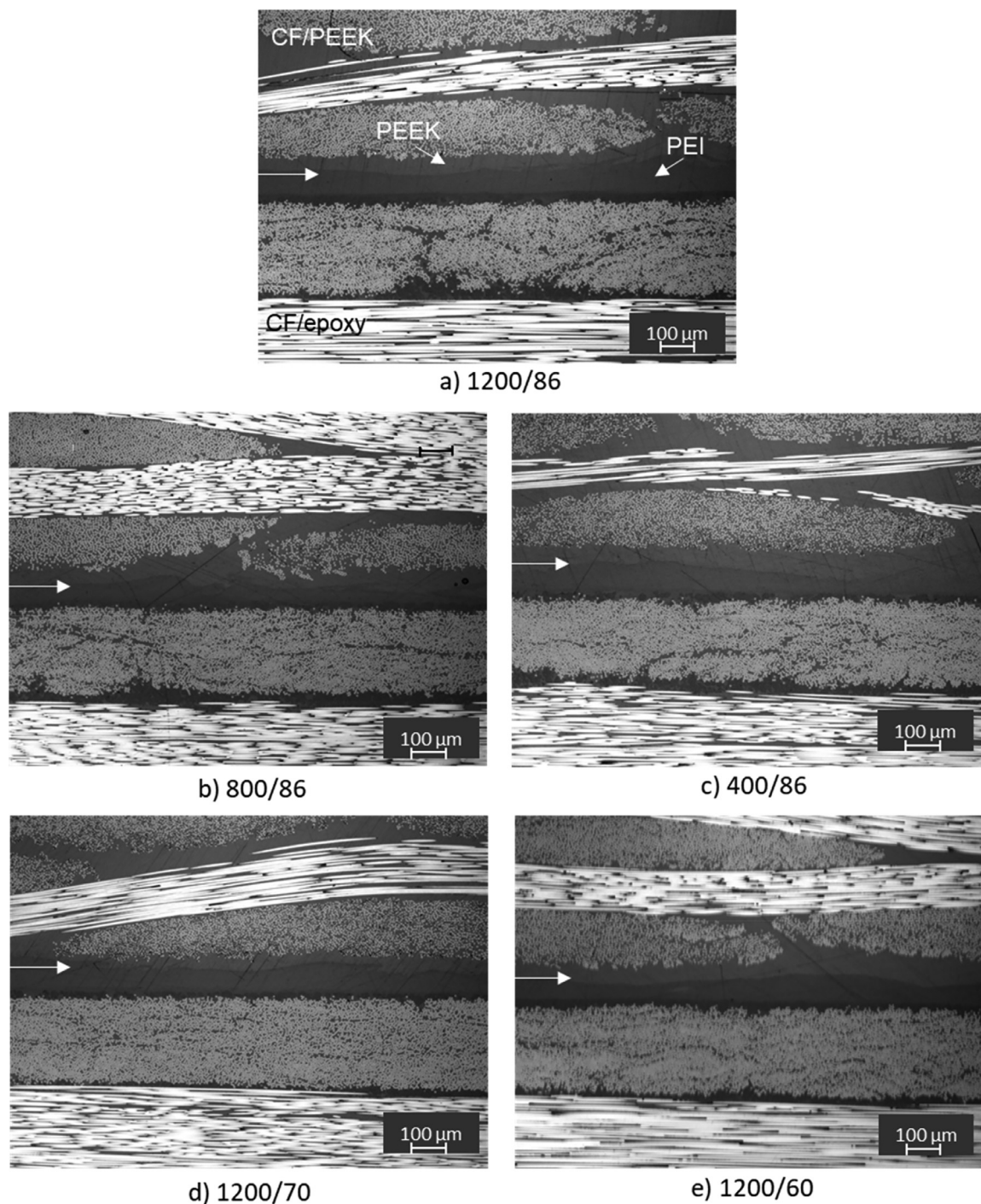


Fig. 12. Cross-sectional micrographs of representative specimens welded in different force/amplitude configurations and at the displacement value that resulted in maximum LSS: a) 1200/86 (0.24 mm), b) 800/86 (0.24 mm), c) 400/86 (0.16 mm), d) 1200/70 (0.24 mm) and e) 1200/60 (0.24 mm), Arrows indicate the resin-rich weld line between the two composite materials.

the maximum temperature (both at the d_{ms} as well as the displacement used in Fig. 5). On the other hand, further decreasing the force from 800 N to 400 N caused a decrease in the maximum temperature. Two could be the reasons for this apparently inconsistent behavior. Firstly, changing from 1200 N to 800 N welding force did not seem to affect the time until onset of squeeze flow at the welding interface but it did affect the squeeze flow rate (Fig. 3). Note that in this particular study, both the energy director and the coupling layer experienced squeeze flow, as evidenced by the decreased thickness and the somewhat wavy

boundary between the two polymers evidenced in the cross-section micrographs in Fig. 12. We hence believe that heat generation rates were similar in both cases, as also evidenced by the fact that the temperature curves were overlapping until approximately 250 ms into the welding process (Fig. 5), which roughly corresponds with the time at which onset of squeeze flow occurred (Fig. 3). However, slower squeeze flow of the molten polymer at the welding interface led to higher temperature increase after the onset at 800 N welding force. Secondly, at 400 N welding force a longer time was needed for squeeze flow to occur (Fig. 3),

which indicates slower heat generation. This might be related to increased hammering causing less efficient amplitude transmission to the welding interface(s) and hence less efficient heating during the initial stages of the welding process [21]. It should be noted that the hammering phenomenon is known to be more pronounced when the welding force is low [14], which would explain why it could have been more apparent at 400 N than at 800 N welding force. Less efficient heating could hence be the cause of the decrease in maximum temperatures observed when decreasing the welding force from 800 N to 400 N.

4.2. Amplitude variations (welding at d_{ms})

The effect of decreasing the amplitude had a much more pronounced effect on the heating time than decreasing the welding force (Table 3). However, the maximum achievable LSS did not seem to be significantly affected by the changes in amplitude either (Table 4). As already observed when decreasing the welding force, decreasing the amplitude did cause increased local first-ply failure in the CF/epoxy composite (see Fig. 11). Similarly, the changes in failure were consistent with a gradual increase of the maximum temperature at the interface between the coupling layer and the CF/epoxy adherend (see Table 2 and Fig. 6). The fact that, despite the significantly longer heating times, the effect of lowering the amplitude did not differ much from that of lowering the welding force could be attributed to the decrease in viscoelastic heating rate resulting from decreased amplitude. Indeed, viscoelastic heat generation is proportional to the cyclic strain, or in other words the amplitude, squared [15]. This slower heat generation was evident from the observation that reducing the amplitude mostly affected (increased) the time until the onset of squeeze flow (Fig. 4).

4.3. LSS versus displacement

When looking at the sensitivity of the welding process to variations in the controlling parameter, i.e., displacement of the sonotrode, in the different force and amplitude combinations investigated in this study (Figs. 7 and 8), there are two main apparent effects. Firstly, decreasing the force or the amplitude caused a more severe drop of the LSS beyond d_{ms} . This is linked to the prevalent occurrence of CF/epoxy failure in those instances (Figs. 10 and 11). Secondly, decreasing the welding force seemed to have a more pronounced effect on the LSS versus displacement curves, by shifting the curves to lower displacement values. However, that shift can be firstly linked to the decrease in the initial constant value of the displacement caused by the lowering of the force (Fig. 3). The fact that there was no statistically significant difference in the weld line thickness (according to ANOVA: $F(4,16)=0.47$, $p = 0.75$) also supports the previous statement. The changes in the initial constant displacement values are likely related to a more notorious effect of thermal expansion of the welding stack when the welding force is low (especially evident in the 400/86 configuration).

5. Conclusion

The present study focused on assessing the sensitivity of ultrasonic welding of CF/epoxy to CF/PEEK composites to decreasing either the welding force (from 1200 N to 800 N and 400 N) or the amplitude of vibrations (from 86 μm to 70 μm and 60 μm). As expected, decreasing the welding force or the amplitude generally caused an increase of the heating times required to obtain maximum weld strength, which was attributed to a decrease in the heat generation rates. Additionally, the temperature to which the CF/epoxy material was exposed during welding increased with decreasing force or amplitude. This temperature increase resulted in partial shift of the locus of failure from the CF/PEEK to the CF/epoxy adherend, interpreted as a sign of thermal degradation in the latter. The maximum achievable lap shear strength was insensitive to the above-mentioned changes, but faster degradation of the weld

strength beyond that point was found in all the cases with lower force or amplitude than the reference case.

Declaration of Competing Interest

The authors declare that they have no known competing financial interests or personal relationships that could have appeared to influence the work reported in this paper.

Acknowledgments

This research is part of the European project EFFICOMP that focuses on efficient manufacturing of composite parts. The EFFICOMP project received funding from the European Union Horizon 2020 research and innovation program under grant agreement no. 690802.

Data availability

The raw/processed data required to reproduce these findings cannot be shared at this time due to technical or time limitations.

References

- [1] C. Ageorges, L. Ye, M. Hou, Advances in fusion bonding techniques for joining thermoplastic materials composites: a review, *Compos. Part A Appl. Sci. Manuf.* 32 (2001) 839–857.
- [2] A.P. da Costa, E.C. Botelho, M.L. Costa, N.E. Narita, J.R. Tarpani, A review of welding technologies for thermoplastic composites in aerospace applications, *J. Aerosp. Technol. Manag.* 4 (2012) 255–265.
- [3] I.F. Villegas, R. van Moorleghem, Ultrasonic welding of carbon/epoxy and carbon/PEEK composites through a PEI thermoplastic coupling layer, *Compos. Part A Appl. Sci. Manuf.* 109 (2018) 75–83.
- [4] Jacaruso G.J., Davis G.C., McIntire A.J. Bonding of Thermoset Composite Structures, 1994.
- [5] I.F. Villegas, P.V. Rubio, On avoiding thermal degradation during welding of high-performance thermoplastic composites to thermoset composites, *Compos. Part A Appl. Sci. Manuf.* 77 (2015) 172–180.
- [6] B. Lestriez, J.-P. Chapel, J.-F. Gérard, Gradient interphase between reactive epoxy and glassy thermoplastic from dissolution process, reaction kinetics, and phase separation thermodynamics, *Macromolecules* 34 (2001) 1204–1213.
- [7] S. Deng, L. Djukic, R. Paton, L. Ye, Thermoplastic-epoxy interactions and their potential applications in joining composite structures – a review, *Compos. Part A Appl. Sci. Manuf.* 68 (2015) 121–132.
- [8] E. Tsiangou, S. Teixeira de Freitas, I.F. Villegas, R. Benedictus, Investigation on energy director-less ultrasonic welding of polyetherimide (PEI)-to epoxy-based composites, *Compos. Part B Eng.* 173 (2019) 107014, doi:10.1016/j.compositesb.2019.107014.
- [9] I.F. Villegas, L. Moser, A. Yousefpour, P. Mitschang, H.E.N. Bersee, Process and performance evaluation of ultrasonic, induction and resistance welding of advanced thermoplastic composites, *J. Thermoplast. Compos. Mater.* 26 (2012) 1007–1024, doi:10.1177/0892705712456031.
- [10] A. Benatar, R.V. Eswaran, S.K. Nayar, Ultrasonic welding of thermoplastics in the near-field, *Polym. Eng. Sci.* 29 (1989) 1689–1698, doi:10.1002/pen.760292311.
- [11] I.F. Villegas, Ultrasonic welding of thermoplastic composites, *Front. Mater.* 6 (2019) 1–10, doi:10.3389/fmats.2019.00291.
- [12] I.F. Villegas, B. Valle Grande, H.E.N. Bersee, R. Benedictus, A comparative evaluation between flat and traditional energy directors for ultrasonic welding of CF/PPS thermoplastic composites, *Compos. Interfaces* 22 (2015) 717–729, doi:10.1080/09276440.2015.1053753.
- [13] Z. Zhang, X. Wang, Y. Luo, Z. Zhang, L. Wang, Study on heating process of ultrasonic welding for thermoplastics, *J. Thermoplast. Compos. Mater.* 23 (2010) 647–664.
- [14] A. Levy, S. Le Corre, I.F. Villegas, Modeling of the heating phenomena in ultrasonic welding of thermoplastic composites with flat energy directors, *J. Mater. Process. Technol.* 214 (2014) 1361–1371, doi:10.1016/j.jmatprotec.2014.02.009.
- [15] I.F. Villegas, In situ monitoring of ultrasonic welding of thermoplastic composites through power and displacement data, *J. Thermoplast. Compos. Mater.* 28 (2015) 66–85.
- [16] F. Lionetto, M.N. Morillas, S. Pappadà, G. Buccoliero, I.F. Villegas, A. Maffezzoli, A Hybrid welding of carbon-fiber reinforced epoxy based composites, *Compos. Part A* 104 (2018) 32–40.
- [17] E. Tsiangou, S. Teixeira de Freitas, I.F. Villegas, R. Benedictus, Ultrasonic welding of epoxy- to polyetheretherketone- based composites: investigation on the material of the energy director and the thickness of the coupling layer, *J. Compos. Mater.* 54 (2020) 3081–3098.

- [18] E. Tsiangou, J. Kupski, S. Teixeira de Freitas, I.F. Villegas, R. Benedictus, On the sensitivity of ultrasonic welding of epoxy- to polyetheretherketone (PEEK)-based composites to the heating time, *Compos. Part A Appl. Sci. Manuf.* 144 (2021), doi:[10.1016/j.compositesa.2021.106334](https://doi.org/10.1016/j.compositesa.2021.106334).
- [19] L. Torre, J.M. Kenny, Blends of semicrystalline and amorphous polymeric matrices for high performance composites, *Polym. Compos.* 13 (1992) 380–385, doi:[10.1002/pc.750130507](https://doi.org/10.1002/pc.750130507).
- [20] M. Abouhamzed, J. Sinke, Effects of fusion bonding on the thermoset composites, *Compos. Part A Appl. Sci. Manuf.* 118 (2019) 142–149, doi:[10.1016/j.compositesa.2018.12.031](https://doi.org/10.1016/j.compositesa.2018.12.031).
- [21] G. Palardy, H. Shi, A. Levy, S. Le Corre, I. Fernandez Villegas, A study on amplitude transmission in ultrasonic welding of thermoplastic composites, *Compos. Part A Appl. Sci. Manuf.* 113 (2018) 339–349, doi:[10.1016/j.compositesa.2018.07.033](https://doi.org/10.1016/j.compositesa.2018.07.033).